Chinese Journal of
POLYMER SCIENCE

ARTICLE

https://doi.org/10.1007/s10118-018-2032-z
Chinese J. Polym. Sci. 2018, 36, 576–583

A Biomimetic Surface for Infection-resistance through Assembly of Metal-phenolic Networks

Ru-Jian Jiang[a, b], Shun-Jie Yan[c], Li-Mei Tian[a], Shi-Ai Xu[b], Zhi-Rong Xin[b*], Shi-Fang Luan[c], Jing-Hua Yin[c], Lu-Quan Ren[a], and Jie Zhao[a*]

[a] *Key Laboratory of Bionic Engineering, Ministry of Education, Jilin University, Changchun 130022, China*
[b] *School of Chemistry and Chemical Engineering, Yantai University, Yantai 264005, China*
[c] *State Key Laboratory of Polymer Physics and Chemistry, Changchun Institute of Applied Chemistry, Chinese Academy of Sciences, Changchun 130022, China*

Electronic Supplementary Information

Abstract Despite the fact that numerous infection-resistant surfaces have been developed to prevent bacterial colonization and biofilm formation, developing a stable, highly antibacterial and easily produced surface remains a technical challenge. As a crucial structural component of biofilm, extracellular DNA (eDNA) can facilitate initial bacterial adhesion, subsequent development, and final maturation. Inspired by the mechanistic pathways of natural enzymes (deoxyribonuclease), here we report a novel antibacterial surface by employing cerium (Ce(IV)) ion to mimic the DNA-cleavage ability of natural enzymes. In this process, the coordination chemistry of plant polyphenols and metal ions was exploited to create an *in situ* metal-phenolic film on substrate surfaces. Tannic acid (TA) works as an essential scaffold and Ce(IV) ion acts as both a cross-linker and a destructor of eDNA. The Ce(IV)-TA modified surface exhibited highly enhanced bacteria repellency and biofilm inhibition when compared with those of pristine or Fe(III)-TA modified samples. Moreover, the easily produced coatings showed high stability under physiological conditions and had nontoxicity to cells for prolonged periods of time. This as-prepared DNA-cleavage surface presents versatile and promising performances to combat biomaterial-associated infections.

Keywords Antibacterial surface; Metal-phenolic coating; DNA-cleavage; Biomimetic surface

Citation: Jiang, R. J.; Yan, S. J.; Tian, L. M.; Xu, S. A.; Xin, Z. R.; Luan, S. F.; Yin, J. H.; Ren, L. Q.; Zhao, J. A Biomimetic Surface for Infection-resistance through Assembly of Metal-phenolic Networks. Chinese J. Polym. Sci. 2018, 36(5), 576–583.

INTRODUCTION

Microbial biofilm formation on the surfaces of medical devices is considered as the main cause of the increased risks associated with life-threatening infections. Bacterial contamination of an implant can occur per- and postoperatively[1]. Upon adhesion, the bacterial phenotype changes, leading to the formation of a biofilm—an organized community of adherent bacteria embedded in a matrix of extracellular polymeric substances (EPS)[2]. Compared to planktonic bacteria of the same species, the embedded cells in biofilm show a reduced susceptibility to the most antimicrobial agents and can survive under harsh conditions, which lead to devastating complications with high costs of treatment[3].

Various strategies have been employed in developing various antibacterial surfaces to prevent the initial bacterial adhesion and subsequent biofilm formation. According to different antibacterial mechanisms, the functionalized surfaces can be divided into bacterial anti-adhesive surfaces (*e.g.* hydrophilic antifouling surfaces[4] and hierarchical superhydrophobic surfaces[5]) and bactericidal surfaces (*e.g.* cationic quaternary ammonium compound (QAC) based coatings[6] and antimicrobial peptides[7]). However those conventional antibacterial strategies have many inherent disadvantages. As for the bacterial anti-adhesive surfaces, once bacteria have irreversibly attached, the passive nature hardly kills the attached bacterial cell and fails to prevent the biofilm formation. As for the bactericidal approach, high cytotoxicity and short-term antibacterial effects have greatly limited their widespread applications[2].

There is increasing evidence that as the longest molecule in EPS, extracellular DNA (eDNA) plays a crucial role in bacterial adhesion and biofilm formation[8]. eDNA, originating either from lysed cells in a biofilm or being released *via* vesicles by metabolically active bacteria, can facilitate the initial bacterial adhesion and connect bacteria with other EPS components to form mature networks[9]. Hence, attacking and cleaving the bacterial eDNA provide a new method to prevent device-related bacterial infections. Whitchurch *et al.*[10] first reported that deoxyribonuclease (DNase) could nonspecifically cleave DNA and inhibit biofilm formation in growth medium; in addition, rinsing a biofilm with DNase could effectively disintegrate 60 h old

* Corresponding authors: E-mail xinzhirong2012@126.com (Z.R.X.)
E-mail jiezhao@jlu.edu.cn (J.Z.)
Received July 17, 2017; Accepted August 30, 2017; Published online January 11, 2018

© Chinese Chemical Society
Institute of Chemistry, Chinese Academy of Sciences
Springer-Verlag GmbH Germany, part of Springer Nature 2018

biofilm. Swartjes *et al.*[8] and our group[11] investigated the antimicrobial efficacy of the covalently immobilized DNase coating in nature. However, low operational stability, high environmental sensitivity, and excessive cost of natural DNase greatly compromise the long-term antibacterial activity of the DNase based surfaces.

Inspired by the mechanistic pathways of natural enzymes, researchers found that synthetic biocatalysts based on Lewis acidic metal ions, such as Ce(IV), Cu(II), and Zn(II), as nuclease mimics could be used to accelerate the hydrolysis of DNA[12–14]. Chen *et al.*[15] and our previous work[16] introduced a DNase-mimetic artificial enzyme based on cerium(IV) ion complexes into a nanoparticle or polymer film surface for combating bacterial attachment and biofilm formation. The synthetic biocatalyst functionalized surfaces exhibited high activity in preventing bacterial adhesion and biofilm formation for prolonged periods of time. However, these techniques often require multi-step treatments involving surface amination, chemical grafting or polymerization, which might be time-consuming or high-cost; in addition, the complex shaped substrates are also restricted.

Polyphenols are widely distributed in many plant tissues, such as green tea, fruits, cocoa, and red wine[17]. Due to the robust anchoring and coordinating ability on various substrates, plant-derived polyphenols have recently attracted significant interest in materials science[18]. Generally, the accepted interfacial bonding mechanism of polyphenol consists of initial substrate surface immobilization of polyphenol molecules or small metal-phenolic complexes and subsequent cross-linking leading to metal ions complexation[19, 20].

In this work, to construct a stable and effective antibacterial surface, tannic acid (TA) and cerium(IV) ion were chosen as representative polyphenol and metallic cross-linker, respectively. Fe(III)-TA coated sample was also prepared as a control to demonstrate the characteristic antibacterial effect of Ce(IV)-TA coated surface. To our knowledge, this novel biomimetic antibacterial Ce(IV)-TA coated surface for combating bacterial adhesion and biofilm formation without the introduction of bactericidal agents and hydrophilic components has not yet been reported. Therefore, we believe that our innovative work offers an environmentally friendly, low-cost and more practical method to inhibit medical device related infections.

EXPERIMENTAL

Materials

Poly(styrene-*b*-(ethylene-*co*-butylene)-*b*-styrene) (SEBS) (Kraton G 1652) with 29 wt% styrene was kindly supplied by Shell Chemicals (USA). Quartz slides were obtained from Zhejiang Lijing Tech Co., Ltd. (Zhejiang, China). Tannic acid (TA, MW = 1701.23 Da) and trimethylchlorosilane were purchased from Sigma-Aldrich (USA). Ceric ammonium nitrate ($Ce(NH_4)_2(NO_3)_6$) and iron(III) chloride hexahydrate ($FeCl_3 \cdot 6H_2O$) were provided by Aladdin-Reagent (China). Gram-negative *Escherichia coli* (*E. coli*; ATCC 25922), Gram-positive *Staphylococcus aureus* (*S. aureus*; ATCC 6538), Luria-Bertani (LB) broth, and phosphate buffered solution (PBS; 0.1 mol/L, pH = 7.4) were obtained from Dingguo Biotechnology Co., Ltd. (China). The LIVE/DEAD Backlight Bacterial Viability Kit L7012 was purchased from Molecular Probe Inc. (USA). All other reagents were of analytical grade and used as received.

Preparation of Ce(IV)-TA Film

Quartz plates (1 cm × 3 cm) and SEBS films (1.2 cm × 0.8 cm) were chosen as primary substrates. Prior to surface modification, the quartz substrates were immersed into a freshly prepared "piranha solution" (1/3 *V*/*V*, 30 vol% H_2O_2/concentrated H_2SO_4, Caution! Piranha solution is highly oxidizing and corrosive! Extreme care should be taken during preparation and use.) at 110 °C for 30 min, then rinsed with distilled water, dried under a stream of nitrogen. Although the formation of metal-phenolic films is independent of substrates[21], hydrophobic surfaces can facilitate the formation of stable metal-phenolic films due to the hydrophobic interaction between substrates and phenyl rings of TA molecule[22]. Therefore, the piranha-treated quartz substrates were placed into 30 mL of anhydrous dichloromethane solution containing trimethylchlorosilane (4 vol%) for 4 h to generate relatively hydrophobic surfaces, followed by rinsing thoroughly with ethanol and distilled water, and drying with nitrogen flow.

Initially, SEBS or treated quartz substrates were placed into a tube containing 4 mL of TA aqueous solution (3.2 mg/mL, pH = 8.0). After 1 min exposure, 4 mL of $Ce(NH_4)(NO_3)_6$ aqueous solution (1.6 mg/mL) was injected into the tube, subsequently the solution was vigorously mixed for another 1 min. Then, the substrates were removed and rinsed thoroughly. This whole process was defined as one coating cycle. This coating process was repeated different times to get the samples with different labeled cycles (1 to 7 coating cycles). Under similar procedure, quartz plates or SEBS film solely treated by TA worked as controls. In addition, as a reference, Fe(III)-TA film was also prepared according to the previous literature[19].

Aqueous Stability of Ce(IV)-TA Film

Dissolution test was conducted by determining the concentration of TA in water over time. The Ce(IV)-TA coated SEBS substrates were submerged in a cell containing 10 mL aqueous solution with different pH values (pH = 1.0, 5.5, 7.4, and 10.0) at room temperature for different incubation periods (24 , 72, and 120 h). Then the substrates were removed and the suspensions were measured by UV-Vis optical absorption spectra.

Characterization

X-ray photoelectron spectroscopy (XPS; VG Scientific ESCA MK II Thermo Avantage V 3.20 analyzer) with an Al Kα source ($h\nu$ = 1486.6 eV) was used to analyze the elemental composition of the surfaces. The bonding energy was detected from 0 eV to 1200 eV and high-resolution spectra were collected with a pass energy of 20 eV and a step size of 0.05 eV. The chemical composition variation of every coating cycle was measured by energy dispersive X-ray spectroscopy (EDS) performed in SEM (Field emitted scanning electron microscopy, XL 30 ESEM FEG, FEI Company, USA). ATR-FTIR spectra were obtained from a Fourier transform infrared spectrometer (FTIR; BRUKER

https://doi.org/10.1007/s10118-018-2032-z

Vertex 70) in attenuated total reflection (ATR) mode. A total of 32 scans were accumulated with a resolution of 4 cm^{-1} for each spectrum. UV-Vis absorption measurements were conducted on a Lambda 35 UV-Vis spectrophotometer (PerkinElmer, USA). Static water contact angle (WCA) was used to measure the wettability of the samples with a drop shape analysis instrument (DSA; KRÜSS GMBH, Germany) at room temperature. The final average angle was obtained from at least three samples.

Bacterial Adhesion

For the bacterial adhesion assay, *S. aureus* and *E. coli* were incubated on separated LB agar plates at 37 °C for 24 h. A single colony of each bacterium from the agar plate was used to inoculate 25 mL of LB medium at 37 °C overnight with shaking at 120 r/min. The culture suspension was centrifuged at 2700 r/min for 10 min to remove the supernatant, and the deposited bacteria were diluted with sterile PBS solution to obtain a concentration of ~10^8 cells/mL.

Covered with the above bacterial suspension (1 mL), the virgin SEBS, SEBS-TA, SEBS-Fe/TA, and SEBS-Ce/TA samples were placed in 48-well plates. After 3 h incubation at 37 °C, the samples were removed and washed with sterile PBS for three times. The samples were stained by LIVE/DEAD BacLight Bacterial Viability Kit for 15 min in dark and observed by confocal laser scanning microscopy (CLSM; LSM 700, Carl Zeiss) to assess the viability of adherent bacteria on the various samples. With the fluorescent microscopy, viable (appearing green) and dead (appearing red) bacterial cells can be easily distinguished. The percentage of the occupied area of adherent bacteria from the fluorescent images was counted using ImageJ software. The number and morphology of the adherent bacteria were evaluated using field emitted scanning electron microscopy (SEM, XL 30 ESEM FEG, FEI Company, USA). The cultured samples were immobilized by 4% paraformaldehyde for 3 h, then dehydrated with a series of ethanol/water mixtures (30%, 50%, 70%, 90%, and 100%) and coated with platinum prior to SEM observation.

Biofilm Formation

The efficacy of the samples in inhibiting biofilm formation was assessed after incubation in LB growth medium. The virgin SEBS, SEBS-TA, SEBS-Fe/TA, and SEBS-Ce/TA samples were placed in 48-well plates and incubated by 1 mL of bacterial suspension with growth medium (10^6 cells/mL) at 37 °C for 48 h to allow biofilm growth. The bacteria medium was refreshed every 24 h. For SEM imaging and CLSM observation of adherent bacteria, the samples were subjected to treatments as described above.

Bactericidal Property

The virgin SEBS, SEBS-TA, SEBS-Fe/TA, and SEBS-Ce/TA samples were placed in 48-well plates and incubated by 1 mL of bacterial suspension with growth medium (10^6 cells/mL) at 37 °C. After different incubation periods (0, 3, 6, 9, 12, and 24 h), the above mentioned bacterial suspensions (200 μL) were transferred to 96-well plates for measuring optical density (OD) by a microplate reader (TECAN SUNRISE, Swiss) at 540 nm, with the fresh growth medium as control.

Statistical Analysis

All data are presented as mean ± standard deviation (SD). The statistical significance was assessed by analysis of variance (ANOVA), * ($p < 0.05$), ** ($p < 0.01$), *** ($p < 0.001$). Each result is an average of at least three parallel experiments.

RESULTS AND DISCUSSION

Tannic acid (TA), containing five digalloyl ester groups covalently attached to a central glucose core, is mostly extracted from plants and microorganisms as a natural high molecular weight polyphenol[18]. Three galloyl groups from TA can form highly stable complexes with Ce(IV) ions, allowing each TA molecule to react with Ce(IV) ions to form a cross-linked film[21]. Catechol functionalized molecules and their derivatives have a high affinity for a wide variety of substrate surfaces and can easily adhere to the surfaces through covalent and noncovalent interactions[23]. Therefore, the initial adsorption onto the substrate surfaces is likely attributed to free TA molecules or small Ce(IV)-TA complexes which are subsequently cross-linked by further Ce(IV) complexation[19]. Consequently, a cross-linked metal-organic (Ce(IV)-TA) film could form on various substrates after short-time incubation in the mixture of the TA and Ce(IV) ions aqueous solutions and Ce(IV) ions regardless of their shapes, physical and chemical properties (Fig. S2, in electronic supplementary information, ESI).

Characterization of Ce(IV)-TA film

Using quartz plates as substrates, the growth of Ce(IV)-TA film after each coating cycle was readily monitored by UV-Vis spectrophotometry (Fig. 1). Two absorption bands at 216 and 274 nm can be assigned to the absorption of phenyl groups in TA[20], indicating the successful immobilization of TA on the quartz plate surface. The gradually increased absorbance values of the films evidently proved the growth of the film thickness as the dip-coating cycles increased. Further, the EDS spectra of the films showed a stepwise increase of cerium content with the increased dip-coating cycles, also confirming the growth of the film thickness and the successful anchor for cerium ions (Fig. S3, in ESI). As displayed in insert

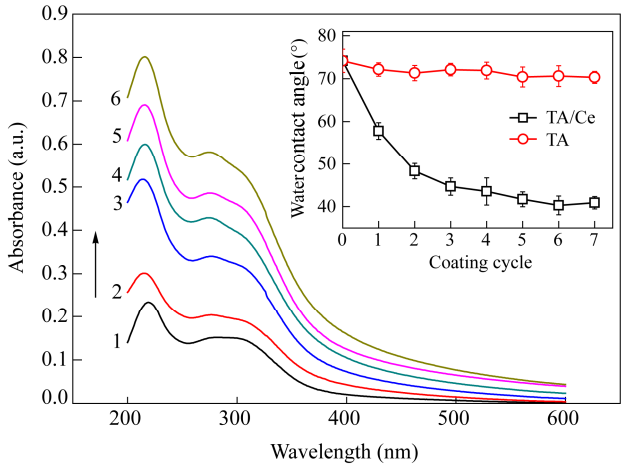

Fig. 1 UV-Vis absorption spectra and water contact angle (inset) of Ce(IV)-TA films with different coating cycles

https://doi.org/10.1007/s10118-018-2032-z

of Fig. 1, the surface showed reduced tendency for water contact angles with increasing Ce(IV)-TA coating cycle and reached a plateau of ~42° after 5 cycles, which was attributed to the fast formation of the Ce(IV)-TA coating on the substrate surface and the surface wettability was almost utterly dominated by the wetting nature of Ce(IV)-TA. In contrast, the quartz plate solely coated by TA showed negligible variation in the surface wettability, revealing that the integrated film could hardly be developed by TA alone within a short-term incubation.

To further verify the successful formation of the Ce(IV)-TA film on other material surfaces, SEBS was chosen as the substrate to get the sample of SEBS-Ce/TA. ATR-FTIR spectra were employed to distinguish the functional groups of films, and the surface chemical compositions of the samples were examined by XPS.

Three new major absorption peaks are observed after SEBS coated with Ce(IV)-TA film (Fig. 2a). The absorption band at 1724 cm^{-1} (shifted from 1716 cm^{-1} to 1724 cm^{-1}) is associated with C=O stretching vibrations of the TA ester groups. The bands at 1342 cm^{-1} (shifted from 1307 cm^{-1} to 1342 cm^{-1}) and 1205 cm^{-1} (shifted from 1177 cm^{-1} to 1205 cm^{-1}) are corresponding to aromatic C—O asymmetrical stretch[24]. The appearance of new bonds at ATR-FTIR spectra confirmed the successful adsorption of TA on SEBS and the obvious red-shift of TA characteristic peaks indicated the coordination of Ce(IV) with TA.

Moreover, the appearance of Ce3d peaks at ~930 eV in SEBS-Ce/TA samples was confirmed by XPS (Fig. 2b red), whereas no cerium signal was discernible on the wide-scan XPS spectrum of virgin SEBS (Fig. 2b black). The results evidently confirmed the successful anchoring of Ce(IV) complexes in SEBS-Ce/TA samples.

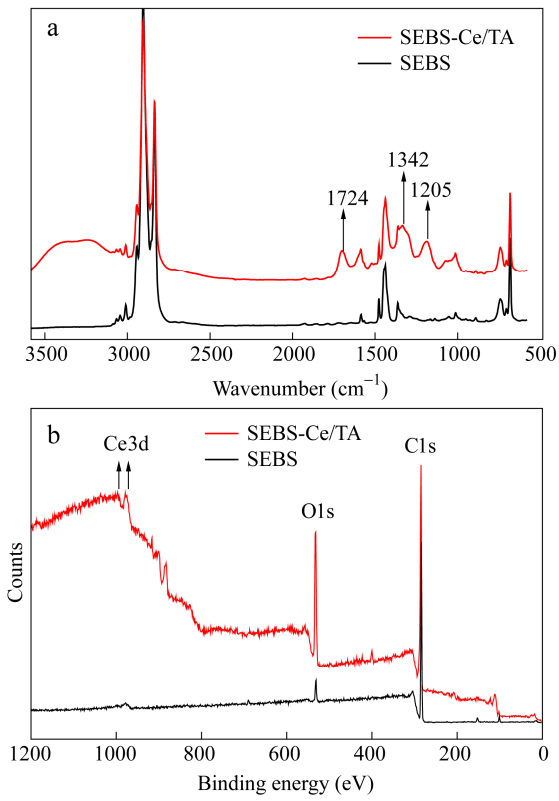

Fig. 2 Representative ATR-FTIR spectra (a) and wide-scan XPS spectra (b) of SEBS (black) and SEBS-Ce/TA (red)

Stability and durability are crucial criteria for evaluating practical applications of the functional Ce(IV)-TA films. The pH-dependent disassembly of Ce(IV)-TA coatings was investigated *via* UV-Vis absorption spectroscopy by placing the SEBS-Ce/TA samples in aqueous solution with different pH values for different incubation periods (Fig. 3). Much weaker absorbance spectra were observed on the disassembled TA aqueous solutions at mild conditions (pH = 5.5 and 7.4) than those at lower (pH = 1.0) or higher pH (pH = 10.0) values with all incubation periods (24, 72, and 120 h).

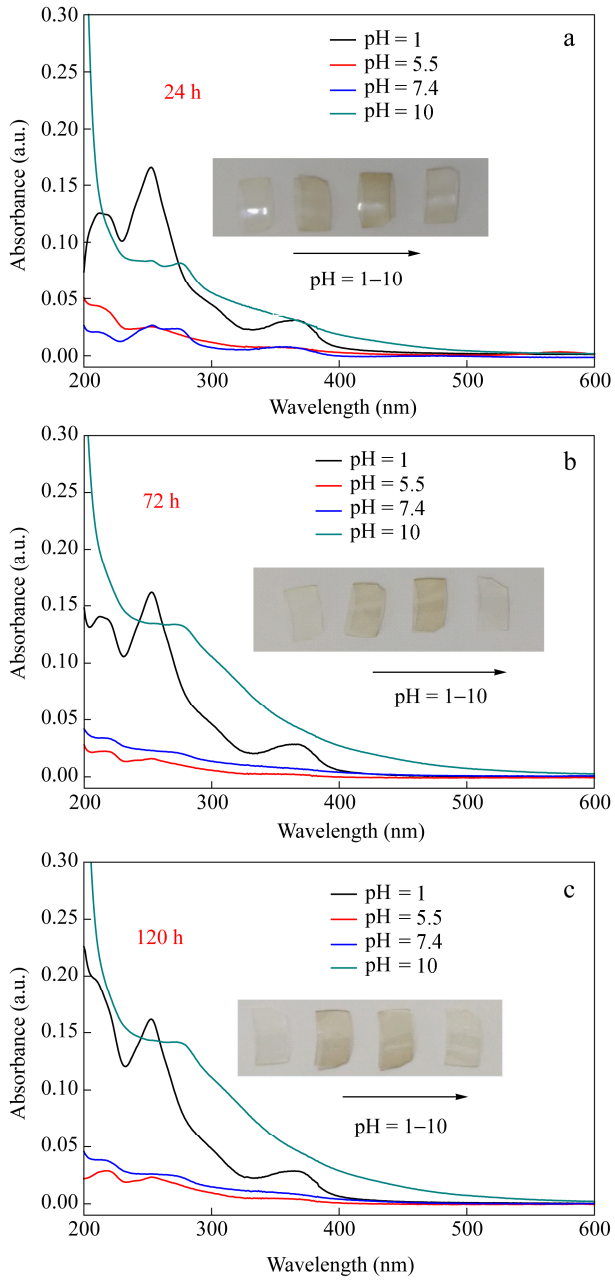

Fig. 3 UV-Vis absorption spectra of disassembled TA after SEBS-Ce/TA samples submerged in various pH aqueous solutions for (a) 24 h, (b) 72 h, and (c) 120 h (The insets are SEBS-Ce/TA samples after solvent immersion. The online version is colorful.)

https://doi.org/10.1007/s10118-018-2032-z

These results clearly demonstrated that the assembled Ce(IV)-TA networks on the SEBS surface were stable enough to undergo long-term incubation time under physiological conditions. In addition, the digital photo analysis provided direct evidences of the stability of SEBS-Ce/TA samples under different pH conditions. As shown in the insert of Fig. 3, the SEBS-Ce/TA samples incubated under aqueous solutions at pH values of 5.5 and 7.4 showed much darker color than the samples under lower or higher pH conditions, even comparable to those prior to incubation. Overall, although the SEBS-Ce/TA might be disassembled under some harsh conditions, these films still maintain their high stability under mild physiological conditions, exerting the inhibition of bacterial-adhesion.

Bacterial Adhesion

The bacterial adhesion, proliferation and colonization on the surfaces have caused severe implant-related infections[25]. Hence, developing an antibacterial adhesive surface is a critical step to prevent subsequent bacterial infection. As a proof-of-concept, Gram-positive *S. aureus* and Gram-negative *E. coli* served as representative bacteria to evaluate the efficacy of the various samples for preventing bacterial initial adhesion. The CLSM images of adherent *S. aureus* and *E. coli* after 3 h of incubation in a PBS buffer (pH = 7.4) are shown in Fig. 4. A great number of viable bacteria with green fluorescence, for both *S. aureus* and *E. coli*, appeared on the virgin SEBS surfaces. Part of the attached bacteria were separated individually, while some were in small clusters, which demonstrated that the surface bacterial adhesion was transforming from an reversible bacterial adhesion to an irreversible bacterial aggregation within 3 h incubation time. Similarly, the samples treated with TA alone hardly exhibited any difference from their virgin counterparts. In comparison, the Fe(III)-TA coated surfaces showed apparently enhanced bacterial resistance, mainly arising from the improvement of surface wettability due to the largely increased hydrophilic groups on the surface. Notably, even more striking bacteria-resistant properties were found on the Ce(IV)-TA coated surfaces when compared to those of Fe(III)-TA, stemming from both the increased hydrophilic groups and the introduction of Ce(IV) ions on the surfaces.

In addition, the corresponding bacterial surface coverage is also illustrated in Fig. 5. The quantitative comparison showed

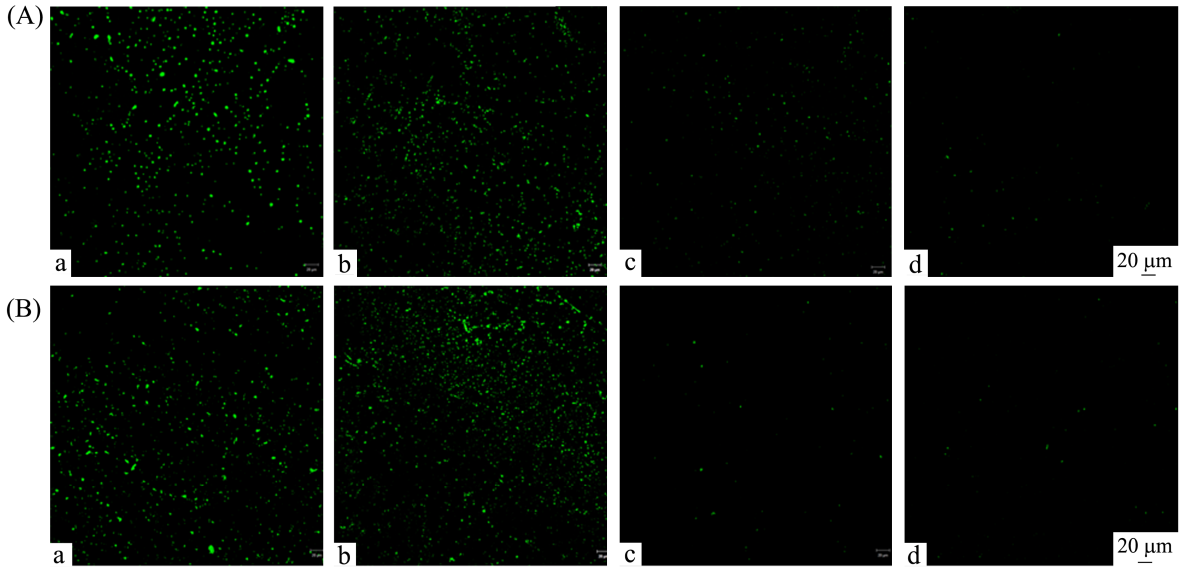

Fig. 4 Representative CLSM images of *S. aureus* (A) and *E. coli* (B) adhesion on virgin SEBS (a), SEBS-TA (b), SEBS-Fe/TA (c), and SEBS-Ce/TA (d) samples after exposure to a PBS suspension of bacteria (10^8 cells/mL) for 3 h (Scale bar is 20 μm.)

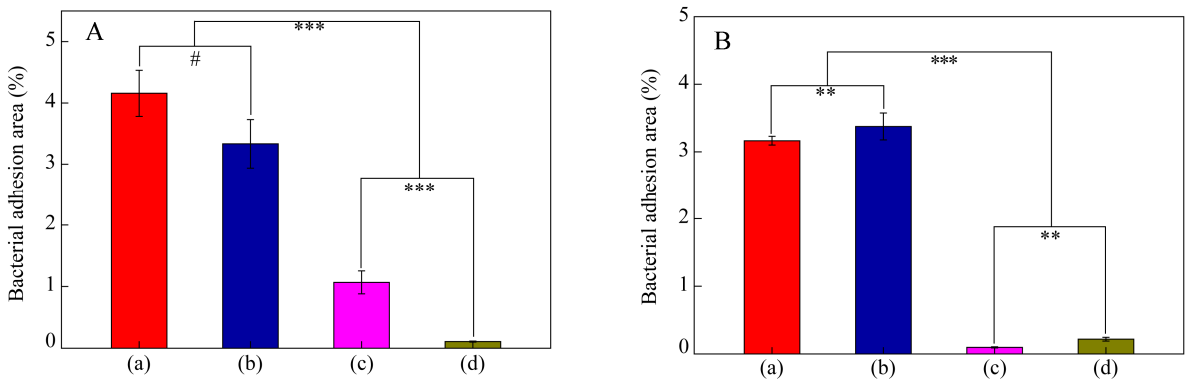

Fig. 5 Percentage of occupied area of adherent *S. aureus* (A) and *E. coli* (B) on virgin SEBS (a), SEBS-TA (b), SEBS-Fe/TA (c), and SEBS-Ce/TA (d) samples after exposure to a PBS suspension of bacteria (10^8 cells/mL) for 3 h (Significant difference * $p < 0.05$; ** $p < 0.01$; ***$p < 0.001$, and # no significant difference.)

https://doi.org/10.1007/s10118-018-2032-z

that bacteria coverage of SEBS-Ce/TA was decreased by ~92.5% for *S. aureus* and ~96.2% for *E. coli* relative to the virgin SEBS reference (Fig. 5). Although the bacterial inhibition activity of TA has been previously reported[26], in our work, SEBS-TA samples failed to show obvious bacterial resistance, as compared to their counterpart of virgin SEBS, mainly due to the failed formation of TA films on surfaces.

Moreover, the cell viability and morphology of bacteria attached to the surfaces were assessed by SEM (Fig. S4, in ESI). The residual bacteria on SEBS-Ce/TA sample maintained their pristine shapes and intact cell surfaces. In addition, no dead cells with red spots were observed in CLSM images (Fig. 4) and all results indicated the fact that SEBS-Ce/TA surface was antibacterial adhesive rather than bactericidal.

Biofilm Formation Evaluation

Biofilms are antibiotic-resistant, sessile bacterial communities that occur on most moist surfaces especially indwelling medical devices. The formation of biofilm provides a protection for cells to survive in hostile environments and also disperses to colonize new niches[27]. It has been confirmed that eDNA plays a pivotal role in maintaining the structural integrity of biofilms through specific and non-specific interaction with bacteria, therefore removal or degradation of eDNA could be an efficient approach to arrest biofilm development and differentiation[11].

Herein, the anti-biofilm activity of SEBS-Ce/TA samples was evaluated by incubation in growth medium (containing 10^6 bacterial cells/mL) for 24 and 48 h. The fluorescent microscopy studies demonstrated that plenty of bacteria was colonized and accumulated on virgin SEBS surfaces for both *S. aureus* and *E. coli* (Figs. 6a1 and 6a2). The percentage of surface coverage on virgin SEBS sample reached ~35.1% and ~46.8% for *S. aureus* and *E. coil*, respectively, after 48 h incubation (Fig. 7). In stark contrast, no obvious biofilms were observed on SEBS-Ce/TA samples after 48 h incubation

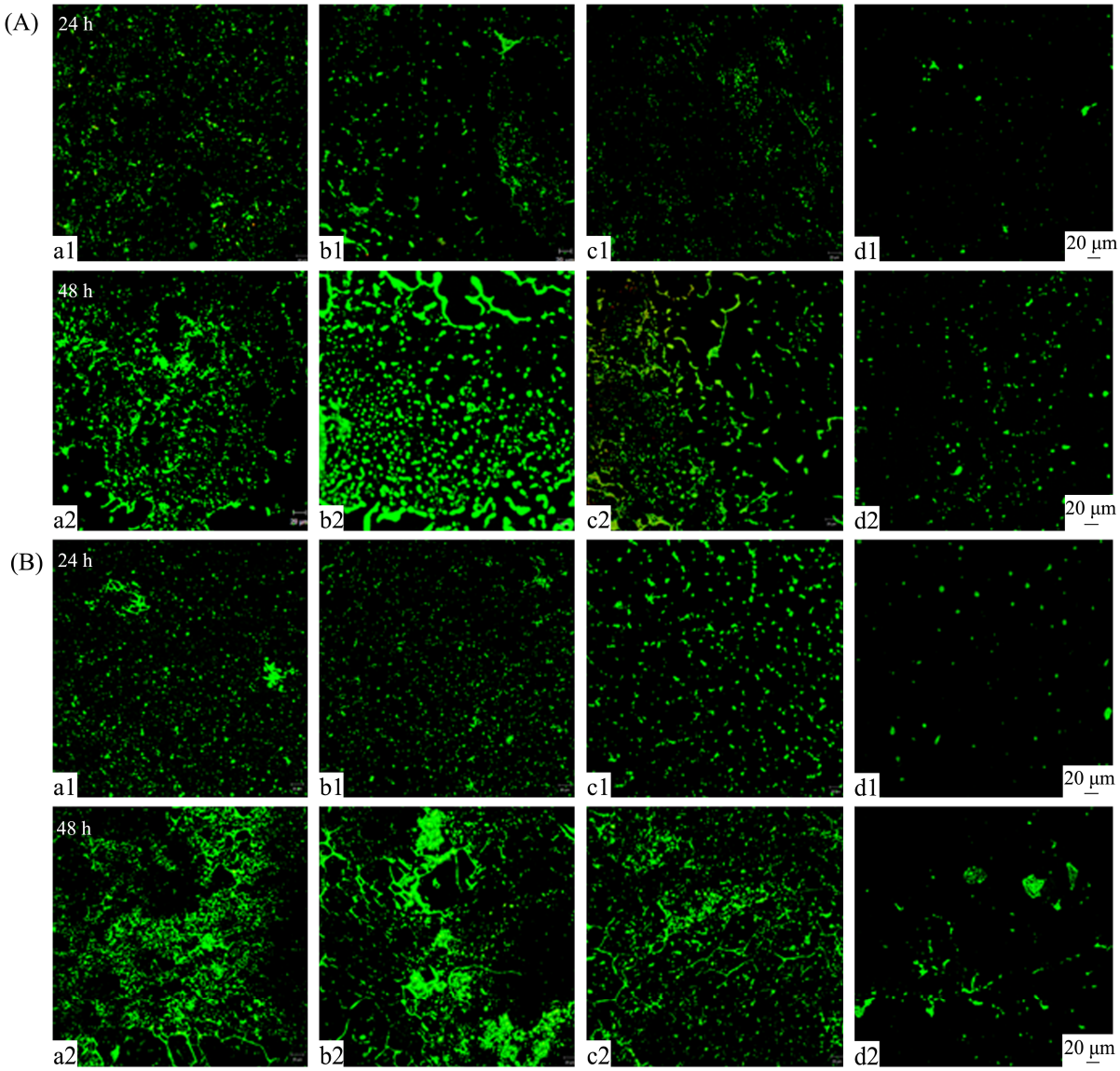

Fig. 6 Representative CLSM images of *S. aureus* (A) and *E. coli* (B) adhesion on virgin SEBS (a1, a2), SEBS-TA (b1, b2), SEBS-Fe/TA (c1, c2), SEBS-Ce/TA (d1, d2) samples after incubation in growth medium containing 10^6 bacterial cells/mL for 24 and 48 h respectively

https://doi.org/10.1007/s10118-018-2032-z

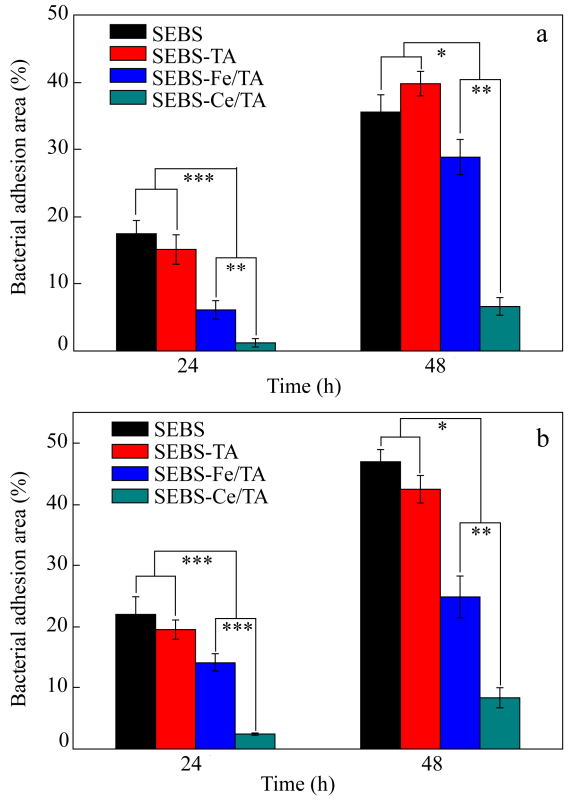

Fig. 7 Percentage of occupied area of adherent *S. aureus* (a) and *E. coli* (b) on various samples after incubation in growth medium containing 10^6 bacterial cells/mL for 24 and 48 h respectively (Significant difference * $p < 0.05$; ** $p < 0.01$; *** $p < 0.001$.)

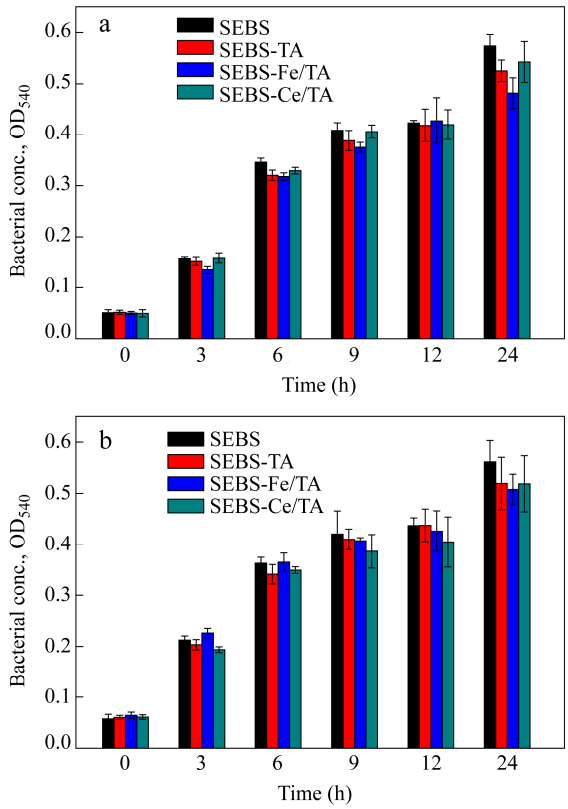

Fig. 8 The vitality of *S. aureus* (a) and *E. coli* (b) after co-incubation with samples in growth medium containing 10^6 bacterial cells/mL for 24 h

(Figs. 6d1 and 6d2). Quantitative image analysis indicated that the bacterial coverage was only ~6.3% and ~7.4% for *S. aureus* and *E. coil*, respectively, with remarkable reductions of ~82.1% and ~84.1% compared to those of virgin SEBS surfaces (Fig. 7). However the reduced bacterial coverage percentages of SEBS-Fe/TA samples were only ~25.3% and ~44.5% for *S. aureus* and *E. coil*, respectively, compared with virgin SEBS after 48 h incubation.

The SEBS-Ce/TA samples demonstrated much higher efficiency for biofilm prevention than Fe(III)-TA films, implying that the DNA-cleavage activity of the Ce(IV) complexes rather than surface hydrophilicity plays a more important role in anti-biofilm activity[15]. Overall, by taking advantage of the eDNA degradation ability and inherent stability of Ce(IV)-TA films, prolonged inhibition of bacterial adhesion and biofilm formation was achieved. SEM observations showed that bacteria readily aggregated and accumulated to form much thicker biofilm structure on the virgin SEBS samples (Fig. S5, in ESI).

Bactericidal Property

To evaluate the toxicity of the few leached cerium ions from Ce(IV)-TA films to bacterial cells, the optical densities (OD) at 540 nm of cultured samples solutions were detected. As shown in Fig. 8, no prominent distinction was observed between virgin SEBS and SEBS-Ce/TA samples at every period for both *S. aureus* and *E. coli*. To further confirm this result, the inhibition of bacterial growth on solid agar plates was also assessed similarly to the traditional Bauer-Kirby method[28]. The experiment was carried out by placing both the SEBS-Ce/TA and a control SEBS upon the bacterial lawns for 24 h. Zone of inhibition tests gave no evidence of any biocidal activity stemming from leached cerium ions with respect to that of other controls (Fig. S6, in ESI), indicating that the Ce(IV)-TA modified surface exerts its antibacterial activity in a way of bacteria repellency rather than bacterial killing.

CONCLUSIONS

In this work, coordination-driven polyphenol coatings that can decorate different substrates were developed by a facile, single-step, low-cost protocol under a mild condition. Surface characterization techniques verified the successful fabrication of Ce(IV)-TA films on different model substrates. The bacteria-repellence and biofilm-inhibition of Ce(IV)-TA films modified surfaces (Biofilm reduction efficiency were ~82.1% and ~84.1% for *S. aureus* and *E. coil*, respectively.) were significantly better than those of the Fe(III)-TA films (Biofilm reduction efficiency were ~25.3% and ~44.5% for *S. aureus* and *E. coil*, respectively.) in a long-term. The excellent antibacterial adhesion of SEBS-Ce/TA surface was attributed to both the enhanced surface hydrophilicity from TA groups and the essential DNA-cleavage activity of the cerium ions anchored on the substrate surface. Therefore, our approach represents a simple, effective and antibiotic-free method to effectively inhibit bacterial attachment and biofilm formation.

https://doi.org/10.1007/s10118-018-2032-z

Electronic Supplementary Information

Electronic supplementary information (ESI) includes details of photographs of aqueous solutions (Fig. S1), spontaneous coatings of Ce(IV)-TA films uncoated or coated on a variety of substrates (Fig. S2.), contents of cerium element after coating cycles on SEBS substrates (Fig. S3), representative SEM images of bacterial adhesion on samples after 3 h incubation (Fig. S4), representative SEM images of bacterial adhesion on samples after 24 h and 48 h incubation (Fig. S5), and photograph of samples of ZOI test against *S. aureus.* (Fig. S6), which is available free of charge in the online version of this article at http://dx.doi.org/10.1007/s10118-018-2032-z.

ACKNOWLEDGMENTS

This work was financially supported by the Research Program Funds of Jilin University (Nos. 419080500665 and 451170301076), and the Natural Science Foundation of Shandong Province (No. ZR2015EM036).

REFERENCES

1 Liu, Y. M.; Li, Q.; Liu, H. H.; Cheng, H. H. Antibacterial thermoplastic polyurethane electrospun fiber mats prepared by 3-aminopropyltriethoxysilane-assisted adsorption of Ag nanoparticles. Chinese J. Polym. Sci. 2017, 35(6), 713–720.
2 Campoccia, D.; Montanaro, L.; Arciola, C. R. A review of the biomaterials technologies for infection-resistant surfaces. Biomaterials 2013, 34(34), 8533–8554.
3 Pozzi, C.; Waters, E. M.; Rudkin, J. K.; Schaeffer, C. R. Methicillin resistance alters the biofilm phenotype and attenuates virulence in *Staphylococcus aureus* device-associated infections. PLoS Pathog. 2012, 8(4), DOI: 10.1371/journal.ppat.1002626
4 Banerjee, I.; Pangule, R. C.; Kane, R. S.; Antifouling coatings: recent developments in the design of surfaces that prevent fouling by proteins, bacteria, and marine organisms. Adv. Mater. 2011, 23(6), 690–718.
5 Banerjee, I.; Pangule, R. C.; Kane, R. S. Antifouling coatings: recent developments in the design of surfaces that prevent fouling by proteins, bacteria, and marine organisms. Adv. Mater. 2011, 23(6), 690–718.
6 Nie, G. H.; Wu, W. J.; Yue, X.; Liao, S. J. Synthesis and properties of hydroxide conductive polymers carrying dense aromatic side-chain quaternary ammonium groups. Chinese J. Polym. Sci. 2017, 35(7), 823–836.
7 Shi, J.; Liu, Y.; Wang, Y.; Zhang, J. Biological and immunotoxicity evaluation of antimicrobial peptide-loaded coatings using a layer-by-layer process on titanium. Sci. Rep. 2015, 5, 16336–16341
8 Swartjes, J. J.; Das, T.; Sharifi, S.; Subbiahdoss, G.; van der Mei, H. C. A functional DNase I coating to prevent adhesion of bacteria and the formation of biofilm. Adv. Funct. Mater. 2013, 23(22), 2843–2849.
9 Das, T., Sehar, S., Manefield, M., The roles of extracellular DNA in the structural integrity of extracellular polymeric substance and bacterial biofilm development. Env. Microbiol. Rep. 2013, 5(6), 778–786.
10 Whitchurch, C. B.; Tolker-Nielsen, T.; Ragas, P. C.; Extracellular DNA required for bacterial biofilm formation. Science 2002, 295(5559), 1487–1487.
11 Yuan, S.; Zhao, J.; Luan, S.; Yan, S.; Nuclease-functionalized poly(styrene-*b*-isobutylene-*b*-styrene) surface with anti-infection and tissue integration bifunctions. ACS Appl. Mater. Interfaces 2014, 6(20), 18078–18086.
12 Komiyama, M.; Takeda, N.; Shigekawa, H.; Hydrolysis of DNA and RNA by lanthanide ions: mechanistic studies leading to new applications. Chem. Commun. 1999, 16, 1443–1451.
13 Li, F. Z.; Xie, J. Q.; Feng, F. M. Copper and zinc complexes of a diaza-crown ether as artificial nucleases for the efficient hydrolytic cleavage of DNA. New J. Chem., 2015, 39(7), 5654–5660.
14 Livieri, M.; Mancin, F.; Saielli, G.; Chin, J. Mimicking enzymes: cooperation between organic functional groups and metal ions in the cleavage of phosphate diesters. Chem. Eur. J. 2007, 13(8), 2246–2256.
15 Chen, Z.; Ji, H.; Liu, C.; Qu, X. A multinuclear metal complex based dnase mimetic artificial enzyme: matrix cleavage for combating bacterial biofilms. Angew. Chem. Int. Ed. 2016, 128(36), 10890–10894.
16 Jiang, R.; Xin, Z.; Xu, S.; Shi, H.; Enzyme-mimicking polymer brush-functionalized surface for combating biomaterial-associated infections. Appl. Surf. Sci. 2017, 423, 869–880.
17 Huang, X. F.; Jia, J. W.; Wang, Z. K.; Hu, Q. L.; A novel chitosan-based sponge coated with self-assembled thrombin/tannic acid multilayer films as a hemostatic dressing. Chinese J. Polym. Sci. 2015, 33(2), 284–290.
18 Quideau, S.; Deffieux, D.; Douat-Casassus, C. Plant polyphenols: chemical properties, biological activities, and synthesis. Angew. Chem. Int. Ed. 2011, 50(3), 586–621.
19 Ejima, H.; Richardson, J. J.; Liang, K.; Caruso, F. One-step assembly of coordination complexes for versatile film and particle engineering. Science 2013, 341(6142), 154–157.
20 Rahim, M. A.; Ejima, H.; Cho, K. L.; Caruso, F. Coordination-driven multistep assembly of metal-polyphenol films and capsules. Chem. Mater. 2014, 26(4), 1645–1653.
21 Guo, J.; Ping, Y.; Ejima, H.; Alt, K.; Caruso, F. Engineering multifunctional capsules through the assembly of metal-phenolic networks. Angew. Chem. Int. Ed. 2014, 53(22), 5546–5551.
22 Yang, L.; Han, L.; Jia, L.; A novel platelet-repellent polyphenolic surface and its micropattern for platelet adhesion detection. ACS Appl. Mater. Interfaces 2016, 8(40), 26570–26577.
23 Lee, H.; Dellatore, S. M.; Messersmith, P. B. Mussel-inspired surface chemistry for multifunctional coatings. Science 2007, 318(5849), 426–430.
24 Han, X.; Zhou, Y.; Hu, J.; Liu, H. Surface modification and characterization of SEBS films obtained by *in situ* and *ex situ* oxidization with potassium permanganate. J. Polym. Sci., Part B: Polym. Phys. 2010, 48(21), 2262–2273.
25 Nejadnik, M. R.; van der Mei, H. C.; Norde, W. Bacterial adhesion and growth on a polymer brush-coating. Biomaterials 2008, 29(30), 4117–4121.
26 Kim, T. J.; Silva, J. L.; Jung, Y. S. Enhanced functional properties of tannic acid after thermal hydrolysis. Food Chem. 2011, 126(1), 116–120.
27 Flemming, H. C.; Wingender, J.; Szewzyk, U.; Kjelleberg, S. Biofilms: an emergent form of bacterial life. Nat. Rev. Microbiol. 2016, 14(9), 563–575.
28 Tamboli, M. S.; Kulkarni, M. V.; Patil, R. H.; Kale, B. B. Nanowires of silver-polyaniline nanocomposite synthesized *via in situ* polymerization and its novel functionality as an antibacterial agent. Colloids Surf. B 2012, 92, 35–41.